Chemical Engineering Science 218 (2020) 115557

Contents lists available at ScienceDirect

Chemical Engineering Science

journal homepage: www.elsevier.com/locate/ces

Novel thermodynamic model for vapor-liquid equilibrium of CO_2 in aqueous solution of 4-(ethyl-methyl-amino)-2-butanol with designed structures

Qiang Li, Hongxia Gao *, Sen Liu, Juan Lv, Zhiwu Liang *

Joint International Center for CO_2 Capture and Storage (iCCS), Provincial Hunan Key Laboratory for Cost-effective Utilization of Fossil Fuel Aimed at Reducing CO_2 Emissions, College of Chemistry and Chemical Engineering, Hunan University, Changsha 410082, PR China

HIGHLIGHTS

- The equilibrium CO_2 solubility of EMAB with designed structures was measured.
- The pKa, reaction kinetics, and heat of CO_2 absorption of EMAB were evaluated.
- Two novel models, i.e. Fugacity-activity and Extended C_f model, are established.
- EMAB is a potential CO_2 capture agent for use in amine-based PCC technology.

ARTICLE INFO

Article history:
Received 6 November 2019
Received in revised form 4 February 2020
Accepted 7 February 2020
Available online 8 February 2020

Keywords:
EMAB
Thermodynamic model
CO_2 capture
Equilibrium solubility
Absorption heat

ABSTRACT

The aim of this project was to develop a thermodynamic model for the vapour-liquid equilibrium of an amine-water-carbon dioxide system and to evaluate the CO_2 capture performance of aqueous EMAB solution. The structurally modified tertiary amine 4-(ethyl-methyl-amino)-2-butanol (EMAB) was chosen because of its molecular structure-activity relationship. Measurements were made of its equilibrium CO_2 solubility, viscosity, dissociation constant, and second-order reaction rate constant, and the heat of absorption was then calculated. Additionally, the novel semi empirical model (Extended C_f model) and the novel rigorous thermodynamic model (fugacity-activity model) which take into consideration the association of the partial molar property and the equation of state were developed to predict the equilibrium CO_2 solubility. The models can provide reasonable prediction results with AARDs of 2.3% and 3.68%, respectively. Furthermore, the thermodynamic and dynamic properties of EMAB were analyzed and evaluated by a comprehensive method and compared with some new tertiary amines and traditional commercial amines. The study concludes that EMAB has good CO_2 capture performance and is expected to be one of the most promising alternative amines for post combustion CO_2 capture technology.

1. Introduction

The carbon dioxide concentration in the atmosphere has been regarded as a key factor contributing to the atmospheric greenhouse effect (Mann et al., 1998; Tokarska and Gillett, 2018). Industrial and coal fired power plants are considered to be the most important sources of carbon dioxide emissions (Zhou et al., 2016). Presently, the amine-based post combustion CO_2 capture technology is considered to be one of the most suitable technologies to reduce CO_2 emissions owing to recent progress in CO_2 removal efficiency improvements, CO_2 purity, and sound economic effectiveness (Liang et al., 2015). However, the application of the individual traditional amine solutions, e.g. MEA (84.3 kJ/mol), DEA (66.9 kJ/mol), and MDEA (54.6 kJ/mol), has been limited by their high energy consumption for CO_2 regeneration while the height of absorber is unchanged. In order to solve the drawbacks of these amines, efforts are being made to develop potential absorbents with better CO_2 capture performance in terms of larger CO_2 capacity, fast reaction kinetics, low reaction heat, better physical properties, and low degradation and corrosion rates.

Moreover, it is crucial to find a new type of structurally modified amine with the potential for utilization. Based on the study of the relationship between amine structure and activity, the novel structurally modified amine with good water solubility, high

* Corresponding author.
E-mail addresses: hxgao@hnu.edu.cn (H. Gao), zwliang@hnu.edu.cn (Z. Liang).

https://doi.org/10.1016/j.ces.2020.115557
0009-2509/

equilibrium CO_2 solubility, faster reaction rate, and environmental friendliness can be designed.

Chakraborty et al. (2002) found by MNDO calculation that the methyl substitution on the α carbon of primary amines and amino alcohols can alter the electron density of the nitrogen atom by reason of the interaction of the π and π* orbitals on the methyl group with the lone-pair orbital of the N atom, thereby causing a lower reaction rate.

Puxty et al. (2009) studied the CO_2 absorption performance of 76 different amines and the experimental results showed that the distance between the hydroxyl functional group and the amino group, and its surrounding structural features seemed to be critical. The amines (i.e. N,N-dimethylethanolamine) with outstanding absorption capacities in common have the structural features of steric hindrance and hydroxyl functionality 2 or 3 carbons from the nitrogen.

Singh et al. (2007, 2009) investigated the relationships of structure and activity for various amines. The results demonstrated that an increase of chain length between the amine and different functional groups decreased the initial absorption rate but increased the absorption capacity in most alkanolamines. Also, alkyl and amine groups were found to be the most suitable functional groups for substitution because both the absorption rate and capacity of the amine were increased.

Singto et al. (2016) focused on the tertiary amine absorbents to evaluate the effect of different functional groups on the CO_2 equilibrium solubility, cyclic capacity, kinetics of absorption and regeneration, and heats of absorption and regeneration. It can be concluded that a tertiary amine with a dimethyl attached to the N atom has higher equilibrium CO_2 solubility and lower ΔH_{abs} due to the shortest alkyl chain length, the smallest steric hindrance and the least electron donating effect; and with diethyl shows a faster reaction rate with CO_2 due to the increase in the electron density of the amine structure.

Recently, the novel tertiary amines, i.e. 4-(dimethylamino)-2-butanol (DMAB) with two methyl groups and 4-(diethylamine)-2-butanol (DEAB) with two ethyl groups, with much higher CO_2 absorption capacities and much larger cyclic capacities compared with conventional MDEA, were shown to be potential absorbents for the capture of CO_2 (Singto et al., 2017). Based on the relationship between structure and activity of amines in the mentioned investigations, the 4-(ethyl-methyl-amino)-2-butanol (EMAB) with one methyl and one ethyl attached to the N atom, with its similar molecular structure to that of DMAB and DEAB, was therefore regarded as a potentially attractive tertiary amine, possibly with high equilibrium CO_2 solubility, high dissociation constant (pKa), fast absorption rate, and low viscosity and CO_2 absorption heat. Thus, EMAB was designed and synthesized in order to verify and investigate its CO_2 capture performance.

Reliable experimental results for the equilibrium CO_2 solubility are indispensable because they can provide vital information for the study of kinetics behavior and the driving forces of gas-liquid mass transfer. Thus, the experimental measurement of equilibrium solubility is essential in absorbent screening. Additionally, the development of theoretical thermodynamic models for vapor–liquid equilibrium (VLE) of amine-water-carbon dioxide systems is also very significant for process design, simulation, and optimization (Rayer et al., 2012). The model requires the incorporation of chemical reactions and physical mass transfer in order to make reasonable predictions based on the VLE experimental data.

It is generally understood that there are several types of vapor-liquid equilibrium models for carbon dioxide-amine-water systems (Téllez-Arredondo and Medeiros, 2013). (i) Semi empirical models are proposed based on the correlation between Raoult's law and Henry's law to calculate vapor-liquid equilibrium. The Kent-Eisenberg model is one such example that has been widely used and successfully applied to predict the vapor-liquid equilibrium in many systems for the equilibrium CO_2 solubility between 0.2 and 0.8 mol CO_2/mol amine (Kent and Elsenberg, 1976). (ii) The excess Gibbs energy model is a more rigorous thermodynamic model due to the introduction of the partial molar property which more closely resembles the real state. The extended Pitzer model, eUNIQUAC model, and eNRTL model based on modified Raoult's law and experimental data are widely used (Aronu et al., 2011; Böttinger et al., 2008; Zhang et al., 2011). (iii) The equation of state (EOS) model is a thermodynamic equation that describes the state of a substance at each physical condition, such as temperature, pressure, volume, and internal energy, and predicts the state of gases and liquids at known conditions. Examples that are increasing in use are the Soave-Redlich-Kwong, Peng-Robinson, and electrolyte EOS models (Diab et al., 2013; Najafloo et al., 2015). Based on the literature survey, it should be noted that it can be of great value to build more accurate semi empirical models with consideration of key factors as well as the thermodynamic models with association of the partial molar property and the equation of state, both of which can reflect the complex behavior of the absorption process under wider thermodynamic conditions and in ternary solvents.

The objective of this work is to synthesize EMAB with high purity; to determine the equilibrium CO_2 solubility in aqueous EMAB solution over the temperature range of 298.15–333.15 K, EMAB concentration of 1–3 mol/L and CO_2 partial pressure of 2.0–101.3 kPa; to measure the viscosity of CO_2 unloaded and loaded aqueous EMAB solutions of 1–3 mol/L at 313.15 K; to measure the dissociation constant pKa at 293.15–318.15 K; to calculate the reaction heat with CO_2 loadings varying from 0.84 to 0.97; and to measure the reaction rate constant for CO_2 absorption in aqueous EMAB solution. Additionally, the equilibrium CO_2 solubility, dissociation constant pKa, and reaction heat of aqueous EMAB solution are evaluated by comparing with more standard amines (i.e. MEA, DEA, and MDEA). Furthermore, the Extended C_f model and novel fugacity-activity model are developed to predict the equilibrium CO_2 solubility, and the AARD was used to estimate the prediction accuracies of the various models.

2. Model theory and description

2.1. Reaction mechanism of CO_2 absorption into aqueous EMAB solution

The base-catalyzed hydration mechanism explanation of the reaction of tertiary amines with CO_2 has been generally recognized and applied by many researchers (Donaldson and Nguyen, 1980; Liu et al., 2019). Based on this reaction mechanism, EMAB only acts as the base for catalyzing the hydration of CO_2 and cannot directly react with CO_2. The chemical reactions of the EMAB-H_2O-CO_2 system can be represented using this mechanism by Fig. 1 and the following Eqs. (1)–(6):

$$EMAB + H^+ \overset{K_1}{\rightleftharpoons} EMABH^+ \quad (1)$$

$$EMAB + CO_2 + H_2O \overset{K_2}{\rightleftharpoons} EMABH^+ + HCO_3^- \quad (2)$$

$$CO_2 + H_2O \overset{K_3}{\rightleftharpoons} H^+ + HCO_3^- \quad (3)$$

$$CO_2 + OH^- \overset{K_4}{\rightleftharpoons} HCO_3^- \quad (4)$$

$$HCO_3^- \overset{K_5}{\rightleftharpoons} CO_3^{2-} + H^+ \quad (5)$$

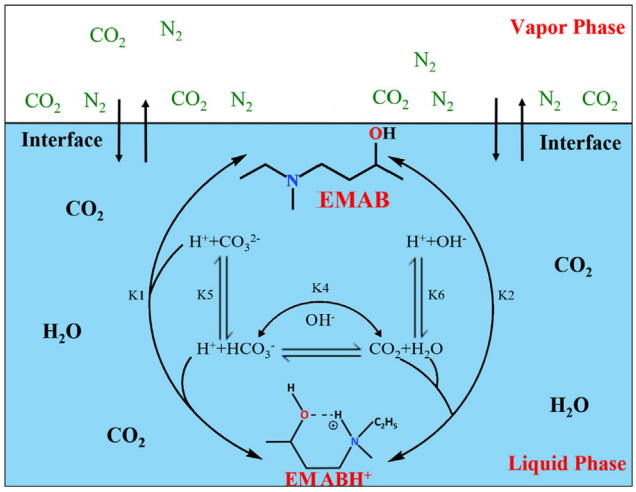

Fig. 1. The chemical reactions and physical transfer of EMAB-H_2O-CO_2 system.

$$H_2O \overset{K_6}{\rightleftharpoons} H^+ + OH^- \tag{6}$$

where K_i (i = 1–6) indicates the chemical equilibrium constant of the above reaction.

The equilibrium constants of each chemical reaction in the EMAB-H_2O-CO_2 system are presented in the following equations:

$$K_1 = \frac{[EMAB][H^+]}{[EMABH^+]} \frac{\gamma_{EMAB}\gamma_{H^+}}{\gamma_{EMABH^+}} \tag{7}$$

$$K_2 = \frac{[EMABH^+][HCO_3^-]}{[EMAB][CO_{2(aq)}]} \frac{\gamma_{EMABH^+}\gamma_{HCO_3^-}}{\gamma_{EMAB}\gamma_{CO_2}} = K_1K_3 \tag{8}$$

$$K_3 = \frac{[H^+][HCO_3^-]}{[CO_{2(aq)}]} \frac{\gamma_{H^+}\gamma_{HCO_3^-}}{\gamma_{CO_2}} \tag{9}$$

$$K_4 = \frac{[HCO_3^-]}{[CO_{2(aq)}][OH^-]} \frac{\gamma_{HCO_3^-}}{\gamma_{CO_2}\gamma_{OH^-}} = \frac{K_3}{K_6} \tag{10}$$

$$K_5 = \frac{[H^+][CO_3^{2-}]}{[HCO_3^-]} \frac{\gamma_{H^+}\gamma_{CO_3^{2-}}}{\gamma_{HCO_3^-}} \tag{11}$$

$$K_6 = \frac{[H^+][OH^-]}{\gamma_{H_2O}} \gamma_{H^+}\gamma_{OH^-} \tag{12}$$

where [i] is the concentration of component i; γ_i stands for the activity coefficient of component i; K_m refers to the equilibrium constant of reaction m; and γ_{H_2O} represents the activity coefficient of water which may be regarded as equal to 1, i.e. γ_{H_2O} = 1. The equilibrium constants of K_2 and K_4 in Eqs. (8) and (10) were calculated from K_1, K_3, and K_6.

Moreover, the system of EMAB-H_2O-CO_2 involves the mass balance of amine and carbon, and total charge balance:

$$[EMAB]_0 = [EMAB] + [EMABH^+] \tag{13}$$

$$\alpha\,[EMAB]_0 = [HCO_3^-] + [CO_3^{2-}] + [CO_{2(aq)}] \tag{14}$$

$$[EMABH^+] + [H^+] = [OH^-] + [HCO_3^-] + 2[CO_3^{2-}] \tag{15}$$

where $[EMAB]_0$ refers to the initial concentration of EMAB; and α stands for the CO_2 solubility (mol CO_2·mol amine^{-1}).

Flue gas is mainly composed of N_2 and CO_2, and the influence of the two gases on the calculation should be considered. The amount of dissolved CO_2 in a solution is proportional to its partial pressure above the liquid according to Henry's law (Xiao et al., 2019).

$$P_{CO_2} \times \varphi_{CO_2} = He \times [CO_2] \times \gamma_{CO_2} \tag{16}$$

where P_{CO_2} refers to CO_2 partial pressure, φ_{CO_2} stands for CO_2 fugacity coefficient, γ_{CO_2} is CO_2 activity coefficient, and He represents Henry's law constant.

2.2. Dissociation constant (pKa)

The dissociation constant pKa is considered to be an indicator of solvent alkalinity and can be used to judge the reaction kinetics of the aqueous amine solution with CO_2 (Brönsted and Guggenheim, 1927). The higher alkalinity of the aqueous amine solution can result in faster reaction kinetics of CO_2 with the amine (Gao et al., 2020). After the formula transformation, Eq. (7) can be converted into the expression Eq. (17), which can be used to calculate the dissociation constant pKa. The detailed process and discussion can be seen in the Supporting Information (S-Table 1).

$$pKa = pH - \log\left(\frac{[Amine]}{[AmineH^+]}\right) - \log\left(\frac{\gamma_{Amine}\gamma_{H^+}}{\gamma_{AmineH^+}}\right) \tag{17}$$

2.3. The fugacity-activity model for CO_2 solubility.

Rigorous thermodynamic models have been proven to be powerful theoretical assets for qualitatively and quantitatively describing the CO_2 absorption mechanisms. In the semi empirical model, the effective concentration and effective partial pressure are ignored. This limits the prediction range and accuracy of the model. Therefore, the fugacity and activity coefficients are introduced to establish a vapor-liquid equilibrium model, that is, the fugacity-activity model. The most significant inputs to the model are the fugacity coefficients and the activity coefficients. The fugacity coefficient of carbon dioxide is calculated with the Virial equation of state, while the temperature, pressure, and composition of the mixed gas are known.

$$\ln\varphi_i = \frac{2}{v}\sum_{j=1}^{m} y_j B_{ij} + \frac{3}{2v^2}\sum_{j=1}^{m}\sum_{k=1}^{m} y_j y_k C_{ijk} - \ln z_{mix} \tag{18}$$

$$z_{mix} = \frac{pv}{RT} = 1 + \frac{B_{mix}}{v} + \frac{C_{mix}}{v} \tag{19}$$

$$B_{mix} = \sum_{i=1}^{m}\sum_{j=1}^{m} y_i y_j B_{ij} \tag{20}$$

$$C_{mix} = \sum_{i=1}^{m}\sum_{j=1}^{m}\sum_{k=1}^{m} y_i y_j y_k C_{ijk} \tag{21}$$

where φ_i represents the fugacity coefficient of component i in the mixed gas; v stands for the molecular volume of the mixture; y_j is the molar fraction of component j; B_{mix} and C_{mix} represents the second and third Virial coefficients of the mixture, independent of pressure or density, and for mixture components are functions of temperature only; the quantity z_{mix} is the compressibility factor; B_{ij} represents the second Virial coefficient corresponding to the i-j interaction and C_{ijk} represents the third Virial coefficient corresponding to the i-j-k interaction.

The third Virial coefficient is more uncertain than the second Virial coefficient because of the pairwise additivity assumption. It should be mentioned that the third Virial coefficient is often omitted due to the mixed gas only containing two molecules. The second Virial coefficient is calculated from the Kihara potential model

(Tee et al., 1966), and the expression for the Kihara potential contains three potential parameters:

$$B_{ij} = 2\pi N_A \int_0^{\infty} \left[1 - e^{\Gamma_{ij}(r)/kT}\right] r^2 dr \tag{22}$$

$$\Gamma = \begin{cases} \infty & r < 2a \\ 4\varepsilon\left[\left(\frac{\sigma-2a}{r-2a}\right)^{12} - \left(\frac{\sigma-2a}{r-2a}\right)^{6}\right] & r \geqslant 2a \end{cases} \tag{23}$$

where N_A is the Avogadro constant; Γ stands for the Kihara potential; a refers to the molecular nucleus; r is the intermolecular distance; ε represents the depth of potential well; and σ represents the collision diameter.

The activity coefficients of EMAB-CO_2-H_2O system are calculated according to the extended Debye–Hückel theory of Deshmukh and Mather (1981).

$$\beta_{ij} = a_{ij} + b_{ij}T \tag{24}$$

$$I = \frac{1}{2}\sum [i] Z_i^2 \tag{25}$$

$$\ln \gamma_i = -\frac{AZ_i^{0.5} I^{0.5}}{1 + 1.2 \times I^{0.5}} + 2\sum \beta_{ij}[j] \tag{26}$$

where β_{ij} refers to the binary specific-interaction coefficient between the solute molecules, i and j. In particular, a_{ij} and b_{ij} are the parameters to be estimated; I stands for the ionic strength of the solution; A represents the Debye-Hückel constant; Z is the charge of component i.

3. Experimental section

3.1. Chemicals

According to the synthetic methods and material on the patent report (Tontiwachwuthikul, 2011), EMAB (wt = 99%) was synthesized as detailed in Fig. 2.

All the EMAB solutions with concentrations of 1–3 mol/L were prepared using deionized water. Nitrogen and carbon dioxide with purities of 99.9% were purchased from Changsha Jingxiang Gas, Co., Ltd., China. The 1 mol/L HCl solution was prepared using 98% hydrochloric acid from Tianjin Komi Chemical Reagent Co., Ltd. Methyl vinyl ketone (MVK, 99%) was provided by cs-pharm Chemical Co., Ltd., Shanghai, China. N-methyldiethanolamine (99%), sodium borohydride (98%), and N-Ethylmethylamine (98%) were all provided by Aladdin Industrial Corporation, Shanghai, China.

3.2. Measurement of equilibrium CO_2 solubility

The apparatus for equilibrium CO_2 solubility measurement as shown in Fig. 3 was employed to measure the VLE of CO_2 in EMAB solution. The apparatus mainly consists of four units, a water saturation unit, a vapor-liquid absorption reactor, a mass flow controller, and a constant temperature water bath (model HANUO, HX20, ±0.05 °C, Shanghai Hannuo Instruments, China), as described in our previous work (Xiao et al., 2016). The main steps are as follows: (i) 20 mL aqueous EMAB solution was added into the vapor-liquid absorption reactor, which was placed in a constant temperature water bath; (ii) the compressed N_2 and CO_2 from the cylinders with desired flow rates controlled by the mass flow controller (model D07, ±1.5% accuracy, Seven Star, China) were mixed by a gas mixer, and then the mixed gas with desired CO_2 partial pressure was introduced into the water saturation unit in order to balance water loss and then the reactor successively; (iii) the system was maintained under operating conditions for at least 12 h to obtain the equilibrium CO_2 solubility. The coiled condenser was used to reduce the loss of EMAB due to volatilization. (iv) Finally, the samples were analyzed using the acid-base titration method to measure and calculation the equilibrium solubility in the system. Each solubility experiment was repeated by two times and each sample was titrated 3–4 times to ensure data repeatability, and the experimental standard uncertainties are 0.004 mol CO_2/mol amine. The measurement of CO_2 loading and calculation of CO_2 solubility can be seen in the Supporting Information S-Fig. 1. This method was put forward by Dreimanis (1962).

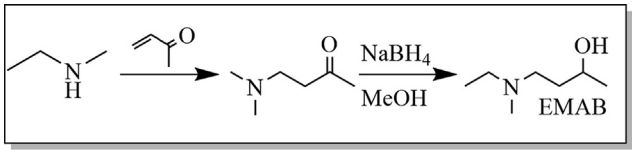

Fig. 2. The molecule structure of 4-(ethyl-methyl-amino)-2-butanol(EMAB).

3.3. Determination of viscosity

A Brookfield viscometer, model DV2T, with accuracy of ± 1.0% of range and repeatability of ± 0.2% was used to measure the viscosities of the amine-H_2O and amine-CO_2-H_2O systems. The temperature was controlled by a constant temperature water bath (model SC-40, Nanjing FINDLAND Technology Co., Ltd, China) with an accuracy of ±0.1 K. Deionized water was used for calibration before each measurement and the measurements were repeated at least 3 times for each sample in order to ensure valid data.

3.4. Determination of dissociation constant (pKa)

Potentiometric titration technique is the most common and quickest experimental technique for amine dissociation constant (pKa) determination (Albert, 2012). The pH meter (±0.01 pH) from PHS-3C Shanghai Lei Magnetic Instrument factory, China was used in the experiments. The detailed experimental procedure based on the method of potentiometric titration to obtain the value of pKa is described in our previous work (Liu et al., 2017b).

4. Results and discussion

4.1. Equilibrium CO_2 solubility of aqueous EMAB solution

Equilibrium CO_2 solubility reflects the maximal absorption capacity of the aqueous amine solution. Generally, the CO_2 partial pressure in the flue gas is very low (about 2 kPa) at the top of the absorber, based on 90% recovery from flue gas with an initial CO_2 partial pressure of 15 kPa. The equilibrium CO_2 solubility at low CO_2 partial pressure is rarely measured in the related studies, but these data are essential to study the absorption performance along the absorber (especially at the top of the absorber) and extend the predicted CO_2 partial pressure range of the vapor-liquid equilibrium model (Rayer et al., 2012).

In this work, all procedures were verified using aqueous MDEA solution, and the measured and reported data can be found in the S-Fig. 2 in the Supporting Information. The equilibrium CO_2 solubility data of 1–3 mol/L aqueous EMAB solutions were determined for the temperature range of 298.15–333.15 K and CO_2 partial pressure of flue gas from 2.0 to 101.3 kPa (Fig. 4), and all the equilibrium CO_2 solubility data can be found in the Supporting Information (S-Tables 2–4). It can be found that the equilibrium CO_2 solubility decreases with the increasing temperature. The explanation for this is that the reaction of CO_2 and amine is a typical reversible and exothermic reaction, which inhibits the progress of the

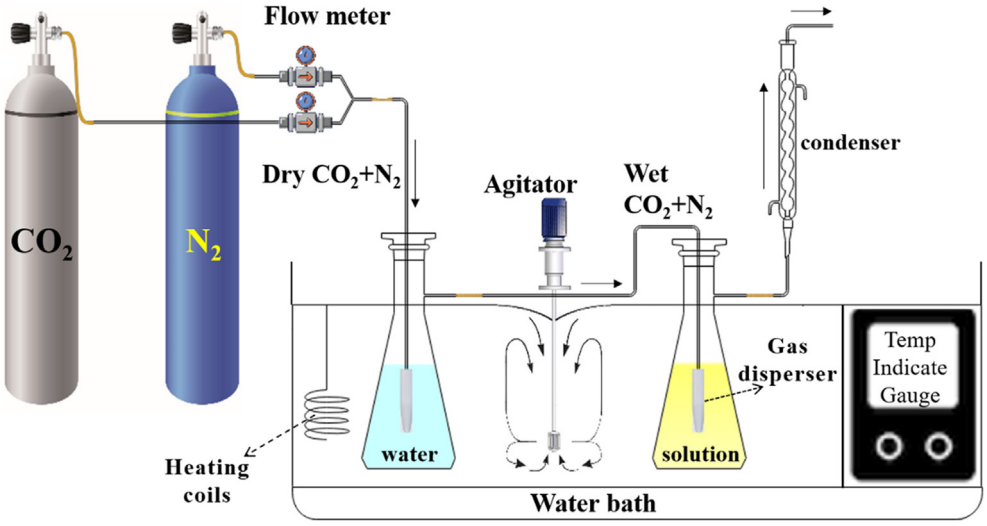

Fig. 3. Schematic diagram of the equilibrium CO_2 solubility measurement.

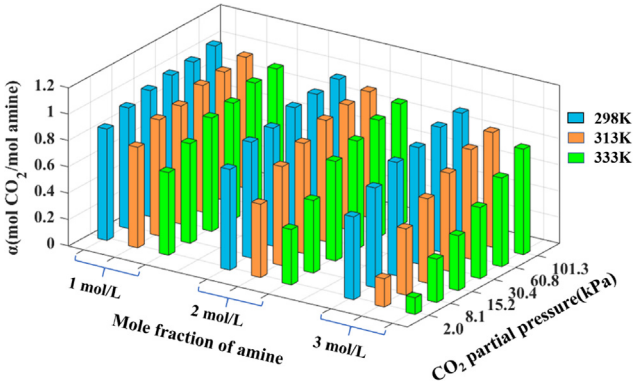

Fig. 4. The equilibrium CO_2 solubility in the aqueous EMAB solution.

reaction as the temperature increases, resulting in a decrease in the equilibrium CO_2 solubility. Looking at Fig. 4, it is apparent that the equilibrium CO_2 solubility increases with the increasing CO_2 partial pressure, and it is worth noting that the equilibrium CO_2 solubility always increases rapidly and then tends to be flat with the increase in CO_2 partial pressure in the low-temperature region (i.e. at 298.15 K). In the high-temperature region (at 333.15 K), the equilibrium CO_2 solubility increases slowly as the CO_2 partial pressure increases. These results indicate that the chemical equilibrium is more sensitive to temperature than CO_2 partial pressure within experimental conditions. This situation is more pronounced as the amine concentration increases due to the decrease of the CO_2/amine molar ratio according to Le Chatelier's principle.

4.2. Viscosity of aqueous EMAB solution

It is well known that the viscosity of solutions is very important to their applicability for CO_2 capture (Alvarez-Fuster et al., 1981). According to the double-membrane theory, this is because increased viscosity results in higher mass transfer resistance that reduces the diffusion and mass transfer rates. Table 1 displays the viscosity of CO_2 unloaded and loaded aqueous EMAB solution with 1–3 mol/L at 313.15 K. It can be found that the viscosity increased with increasing mole fraction and CO_2 loading, and was lower than that of MDEA solution (Shokouhi et al., 2015). It can be concluded that higher the CO_2 loading means higher viscosity for aqueous EMAB solution.

4.3. Dissociation constant (pKa) of aqueous EMAB solution

In order to verify the accuracy of the method of measuring and calculating pKa, the pKa value of the 0.01 mol/L N-methyldiethanolamine (MDEA) solution was measured over the temperature range of 293.15–318.15 K and plotted as a function of reciprocal of temperature (Fig. 5). The measured values obtained for MDEA were in outstanding agreement with those published by Pérez-Salado Kamps et al. (1996) with an AARD of 0.1%, which is acceptable. Then, the dissociation constant of aqueous EMAB solution was measured at different temperatures, and the pKa values are displayed in Fig. 5, clearly showing that the pKa of EMAB solution decreases as the temperature increases. It seems that these results are due to the reaction between the amine molecules and hydrogen ions which was promoted by the increasing temperature, resulting in an increase in basicity in the EMAB solution. Based on the non-linear regression analysis of the pKa values of EMAB solution in Fig. 5, the pKa of aqueous EMAB solution correlated with temperature can be expressed as:

$$\mathrm{pKa} = \frac{2318}{T} + 2.12 \ (R^2 = 0.995) \tag{27}$$

The equilibrium constant K_1 of EMAB with CO_2 in aqueous solutions is of considerable significance to understand the reaction mechanism and to develop the fugacity-activity models. According to the reaction mechanism of EMAB with CO_2, K_1 is unknown among all the independent chemical reaction equilibrium constants. In this study, the value of K_1 was calculated according to the equation $\mathrm{pKa} = -\log(K_1)$, and the equilibrium constant K_1 values are displayed in Fig. 6. It can be found from Fig. 6 that K_1 increases as the temperature increases because of the increase in the protonation ratios. The expression $K_1 = \exp(-5338/T - 4.88)$was obtained by fitting the relationship between the equilibrium constant K_1 at various concentrations and the temperature of EMAB, and this expression can be employed to predict the degree of protonation of an amine in an aqueous solution.

4.4. Vapor-liquid equilibrium (VLE) model for EMAB-CO_2-H_2O system

For the purpose of predicting the equilibrium CO_2 solubility, the thermodynamic model is essential. Particularly, a reliable and accurate correlation for equilibrium constant K_1 (or C_f) as a function of various factors is significant and required. Therefore, the

Table 1
The viscosity of CO_2 unloaded and loaded aqueous EMAB solution with 1–3 mol/L at 313.15 K.

1 mol/L		2 mol/L		3 mol/L	
CO_2 loading (mol CO_2/mol amine)	Viscosity (mPa·s)	CO_2 loading (mol CO_2/mol amine)	Viscosity (mPa·s)	CO_2 loading (mol CO_2/mol amine)	Viscosity (mPa·s)
0	0.97	0	1.71	0	3.24
0.273	1.15	0.285	1.98	0.275	4.56
0.545	1.23	0.570	2.29	0.550	4.96
0.993	1.27	0.955	3.20	0.919	7.74

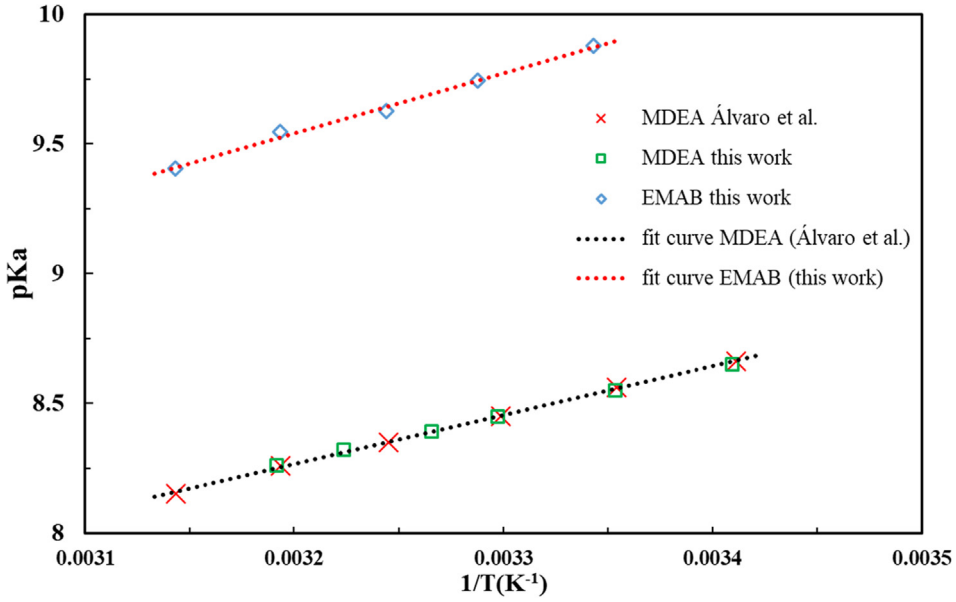

Fig. 5. Dissociation constants of MDEA and EMAB at different temperatures.

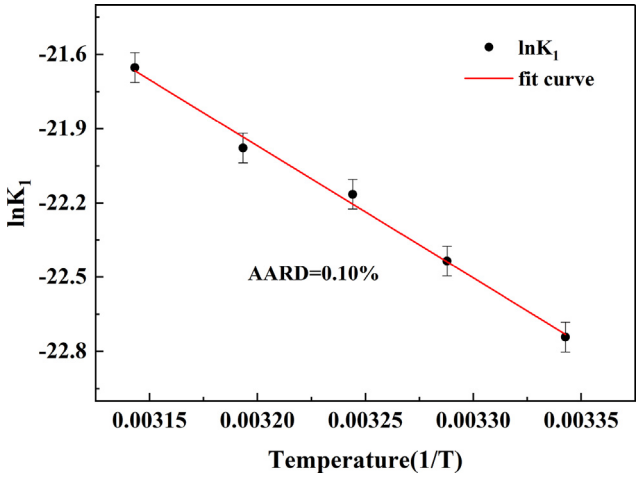

Fig. 6. Equilibrium constant K_1 of EMAB with CO_2 at different temperatures.

equilibrium constant K_1 was fitted by five semi empirical models, namely, KE model, Li-Shen model, Hu-Chakma model, C_f model, and Extended C_f model. The comparison of the newly developed Extended C_f model and the other four semi empirical models was conducted by evaluating the AARD of the experimental and the predicted values of equilibrium CO_2 solubility. Additionally, a novel thermodynamic model, the fugacity-activity model, was also initially proposed based on the combination of the Virial equation and Debye-Hückel theory and estimated to verify the accuracy and the scope of application.

4.4.1. The semi empirical model implementation and estimation of parameters

Five semi empirical models (e.g. KE model, Li-Shen model) were used to predict the equilibrium CO_2 solubility of aqueous EMAB solution. The semi empirical expressions and the corresponding parameters are summarized in Table 2 (Hu and Chakma, 1990; Kent and Elsenberg, 1976; Kundu et al., 2003; Xiao et al., 2017). Kent and Eisenberg have reported a KE model expression which only depends on the temperature. Its modifications are widely used, such as in the Li-Shen and Hu-Chakma models (Hu and Chakma, 1990; Kundu et al., 2003). Additionally, the C_f and Extended C_f models are derived from an assumption for the ideal solution of infinite dilution. It should be noted that the newly developed Extended C_f model has been corrected by introducing equilibrium CO_2 loading data.

In the semi empirical models, the difference between the real state and the ideal state is neglected, and the activity and fugacity coefficients have been considered to be equal to one. The semi empirical models lumped the nonidealities of the amine-CO_2-H_2O system into one model expression to correct non-ideality and reduce deviation. The equilibrium constants (i.e. K_3, K_5, and K_6) of Eqs. (9), (11) and (12) and the Henry's law constant from the reference (Edwards et al., 1978; Kent and Elsenberg, 1976) are presented in S-Table 5 of the Supporting Information. The least-squares regression and non-linear programming solution methods were used to fit the parameters of each model under different conditions, as summarized in Table 3. Also, each model is used to predict the equilibrium CO_2 solubility in aqueous EMAB solution. The accuracies of the five models with regards to AARD can be compared in Fig. 7.

Table 2
Presents a review of five different studies on the semi empirical expressions and their parameters[a].

Model	Model expression	Parameters	Refs
KE	$K_1 = \exp(B_1 + \frac{B_2}{T} + \frac{B_3}{T^2} + \frac{B_4}{T^3} + \frac{B_5}{T^4})$	T	(Kent and Elsenberg, 1976)
Li-Shen	$K_1 = \exp\left(B_1 + \frac{B_2}{T} + \frac{B_3}{T^2} + \frac{B_4}{\alpha} + \frac{B_5}{\alpha^2} + \frac{B_6}{\alpha^{-1}} + B_7 \ln[A]_0\right)$	T, α, $[A]_0$	(Kundu et al., 2003)
Hu-Chakma	$K_1 = \exp(B_1 + \frac{B_2}{T} + B_3 \frac{P_{CO_2}}{He_{CO_2}} + B_4 \ln[A]_0)$	T, P_{CO_2}, He, $[A]_0$	(Hu and Chakma, 1990)
C_f	$C_f = [H^+]/[H^+]^* = \exp(B_1 \ln[CO_2] + B_2 \ln[A]_0 + B_3)$	$[CO_2]_0$, $[A]_0$	(Xiao et al., 2017)
Extended C_f	$C_f = [H^+]/[H^+]^* = \exp(B_1 \ln[A]_0 + B_2/[CO_2] + B_3/\alpha) + B_4$	$[CO_2]_0$, $[A]_0$, α	This work

[a] Where B_i is temperature model parameter, $[A]_0$ is the initial concentration of amine.

The AARDs between the experimental values and predicted data obtained from the KE, Li-Shen, Hu-Chakma, C_f and Extended C_f models are 9.25%, 4.74%, 12.75%, 8.72% and 3.68%, respectively. In comparison, the Extended C_f model is able to predict the equilibrium CO_2 solubility better than the other four models, giving the lowest AARD of 3.68%. In addition, Fig. 7 presents the comparison of experimental equilibrium CO_2 solubility and predicted equilibrium CO_2 solubility of all five models.

The KE model, a simple model only related to the temperature, predicts the equilibrium CO_2 solubility with AARD of 9.25%. However, it was found that most of the predicted data are lower than the measured data, demonstrating the limitation of having only one factor (temperature) considered in the KE model and the necessity of having more factors included. Then, the Li-Shen model (an upgraded version of Kent–Eisenberg model), expressed as the functions of temperature, initial amine concentration and CO_2 loading, was applied to calculate the equilibrium CO_2 solubility. The predicted data are in favorable agreement with the measured equilibrium CO_2 solubility with the lower AARD of 4.74%, leading to better prediction than the KE model as expected. In addition, the Hu-Chakma model (also a modified Kent–Eisenberg model) had been proposed according to the assumption that the chemical equilibrium constant is related to the temperature, the initial amine concentration and the CO_2 partial pressure in the gas phase. However, the predicted results for the EMAB solution were not consistent with the experimental equilibrium CO_2 solubility with an AARD of 12.75%. In the three models above, the Li-Shen model, which considers the CO_2 loading instead of CO_2 partial pressure, shows the lowest deviation in the prediction results for the EMAB solution. The CO_2 loading represented the CO_2 max absorption capacity in the aqueous amine solution, which has a considerable effect on the CO_2 solubility. Thus, the CO_2 loading is an important parameter to predict the equilibrium CO_2 solubility, and thus in the Extended C_f model proposed in this work, the C_f values are expressed as functions of not only CO_2 physical solubility and initial amine concentration, but also of the CO_2 loading. Then, the C_f model and new Extended C_f model corrects the non-ideality in the system by using the correlation parameters adjusted hydrogen ion concentration. The C_f model establishes an expression to correlate C_f values with a function of CO_2 physical solubility and initial amine concentration and predicts the equilibrium CO_2 solubility with AARD of 8.72%. The new Extended C_f model is also an upgraded version of the C_f model and has the lowest AARD at 3.68%. As expected, the novel Extended C_f model showed better prediction ability than did the C_f model with consideration of CO_2 loading.

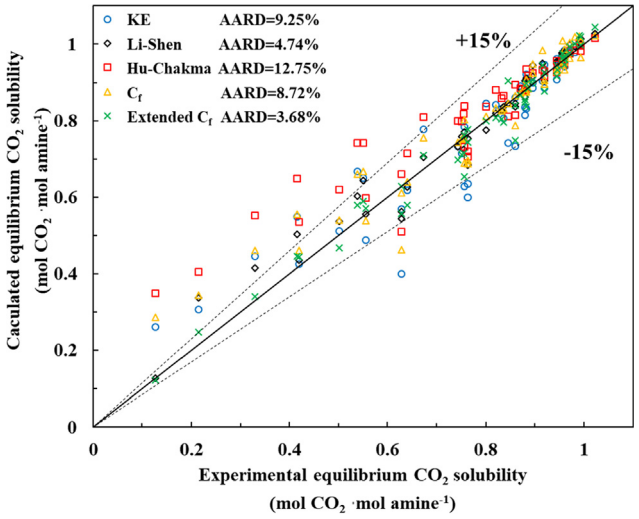

Fig. 7. Calculated equilibrium CO_2 solubility from five semi empirical models versus experimental equilibrium CO_2 solubility.

In addition, Fig. 7 displays the comparison of experimental equilibrium CO_2 solubility and predicted equilibrium CO_2 solubility of all five models. Obviously, except for the Extended C_f model, the results of the models in the low loading area are not ideal. This may be because the low loading area usually corresponds to high temperature and low CO_2 partial pressure, and the non-ideal effect is more obvious in the system. Other models do not have enough ability to correct non ideality. The current study found that the equilibrium CO_2 solubility of EMAB could be better predicted by the semi empirical models which consider the CO_2 loading parameter. However, the semi empirical model may fail to show good predictions under high temperature and low CO_2 partial pressure.

4.4.2. The fugacity-activity model implementation and estimation of parameters

Taking into account the effective partial pressure and effective concentration of the solution, the fugacity-activity model was

Table 3
The parameters values of five semi empirical models.

Model	Parameters						
	B_1	B_2	B_3	B_4	B_5	B_6	B_7
KE	−4.94	−5370	−19.5	1000	1000	–	–
Li-Shen	42.3	−3.43E4	4.36E6	−0.543	7.65E-02	−5.45E-02	1.33
Hu-Chakma	−39.8	5.39E-02	47.4	−0.35	–	–	–
C_f	0.037	0.044	0.126	–	–	–	–
Extended C_f	0.02	0.129	−1.23E-04	−0.153	–	–	–

firstly proposed by introducing the fugacity-activity coefficient based on the Debye-Hückel theory and Virial equation. For the purpose of predicting the equilibrium CO_2 solubility in aqueous EMAB solution, three parameters in the proposed fugacity-activity model, i.e. protonation constant K_1, fugacity and activity, need to be obtained by suitable methods. As mentioned, the protonation constants K_1 can be calculated from the dissociation constant pKa. In this work, fugacity in the gas phase mixture is expressed as the Virial equation (Eq. (18)). The remarkable advantage of using the Virial equation is that the parameters in the equation have clear physical meaning, and the parameters can be directly related to intermolecular forces. The expression of Virial coefficients of pure N_2 and pure CO_2 gases and mixtures have been summarized in a book by Dymond et al. (2003), as shown in Table 4. Then, the fugacity coefficients at various temperatures and CO_2 partial pressure conditions can be calculated by Eqs. (17–19) and (21).

For the calculation of the activity coefficient, the remaining process is to calculate the unknown concentrations of the 7 species (EMAB, $EMABH^+$, CO_2, CO_3^{2-}, HCO_3^-, OH^-, H^+) and optimize the value of the interaction parameters in the investigated system. Because the numerical solution of these activity model equation requires extensive calculation, up to now the estimation of interaction parameters has been seriously hindered. It is, therefore, of prime importance to reduce the computational effort and optimize parameters by reasonable simplifications of the activity calculation.

For this purpose, the underlying assumptions have been set as follows:

(1) Assuming that all binary interaction parameters are symmetrical ($\beta_{ij} = \beta_{ji}$).
(2) Setting all binary interaction parameters between the same charge ions to zero.
(3) Ignoring the effects of low concentrations (H^+ and OH^-) of materials that also have high concentration.

Based on the above assumptions, there are only ten pairs of interacting molecular (ion) pairs in the EMAB solution; that is, only ten pairs of binary interaction parameters are required to be calculated. Fig. 8 displays the detailed calculation progress by using the fugacity-activity model for the EMAB-H_2O-CO_2 system. The "lsqnonlin" function of MATLAB software is used to perform nonlinear data-fitting to obtain the binary interaction parameters.

In the calculation process shown in Fig. 8, the value of binary specific interaction is optimized via iteration until the AARD is minimized to an acceptable value lower than δ (δ = 0.025). The value of δ is determined by multiple trials of the loop body in "lsqnonlin" function, ensuring a good accuracy of solubility prediction. Table 5 presents the optimized ten pairs of binary interaction parameters.

The experimental values and the calculated values of equilibrium CO_2 solubility from the fugacity-activity model are presented in Fig. 9. In the Fig. 9, the dots represent experimental values, and the curves and curved surfaces represent the predicted values by the fugacity-activity model. The curved surfaces of Fig. 9(d) shows the trend of equilibrium solubility in different concentrations of amine solution over a range of 2.0–101.3 kPa CO_2 partial pressure and a temperature range of 298.15–333.15 K. In the range of 0–40.0 kPa CO_2 partial pressure, the trend in Fig. 9 is that the lower the temperature and the amine concentration in the solution investigated, the greater the change in equilibrium CO_2 solubility. Furthermore, Fig. 10 displays the ion speciation plots of EMAB-CO_2-H_2O system at 313.15 K with amine concentrations of 2 mol/L, according to the calculation results of the model.

The predicted values of equilibrium CO_2 solubility obtained from the fugacity-activity model show exceptional correlation with the experimental result at all the operational conditions with AARD of 2.3% (Fig. 11). It is evident that the fugacity-activity model can correctly predict the equilibrium CO_2 solubility in aqueous EMAB solution with only minor deviations by taking into consideration the effective partial pressure and effective concentration of the molecules (ions) in the systems. In addition, the fugacity-activity model can extrapolate the data outside the experimental conditions, because the expression of the protonation constant and the calculation of the fugacity have a wide range of applicability, and the binary interaction parameters of the computational activity depend only on the components in the system. The dashed line in Fig. 9 is the predicted equilibrium CO_2 solubility of the aqueous EMAB solution at 353.15 K. The extrapolation of equilibrium solubility, especially in the case of high amine concentrations and at low CO_2 partial pressure region, is very important for process simulation and process design.

4.4.3. Evaluation and analysis of two types of models

The purpose of this section is to evaluate and analyze the two types of models in order to provide some constructive comments on the development of rigorous thermodynamic models. By comparing Fig. 7 and Fig. 11, it can be found that the fugacity-activity model and the Extended C_f model provide reasonable prediction results with AARDs of 2.3% and 3.68%, respectively. Almost all predicted values are less than 5% deviation, while four semi empirical models give AARDs of 4.74%-12.75% in prediction and some of the predicted values are more than 15% deviation. This shows that the fugacity-activity model and the Extended C_f model can provide reasonable predictive results, and the prediction accuracy is much improved.

For the semi empirical model, the predicted solubility is based on the equilibrium constants of the reactions. The same expression and data of equilibrium constants (K_3, K_5, K_6) and Henry's law constant were used in different amine water systems, resulting in the large deviation between predicted and experimental values (Xiao et al., 2019). Therefore, the accuracy of the predicted results is closely related to the applicability of the equilibrium constant and Henry's law constant in the literature. For the C_f and Extended C_f models, the correction factor was developed to correct the non-ideality of the aqueous amine solution. This method of correcting the non-ideality of the system is simple and effective in the specific range, but the accuracy of predicted results may be affected by many factors (i.e. temperature and pressure range). If the model is applied inappropriately, larger deviation may be observed. In summary, the valid range of the semi empirical model depends on the research systems and experimental conditions.

For the rigorous thermodynamic fugacity-activity model, fugacity and activity are introduced to correct the non-ideality of the mixed gas and aqueous amine solution. The truncated Virial equation was used to calculate the fugacity coefficients, and the parameters in the equation can be directly related to the intermolecular forces. Therefore, the applicability of fugacity is not limited to only one system and can be applied over a wider range of temperatures and pressures. The activity coefficients are calculated by the robust model based on Debye–Hückel theory. Binary interaction parameters are used to make the rigorous thermodynamic fugacity-activity correction of non-idealities in aqueous amine solutions.

Table 4
The Virial coefficients of pure N_2 and CO_2 gases and mixtures.

Molecule	The Virial coefficients	T(K) range
CO_2	$B_{11} = 57.4 - \frac{3.8829E4}{T} + \frac{4.2899E5}{T^2} - \frac{1.4661E9}{T^3}$	220–770
N_2	$B_{22} = 40.286 - \frac{9.3378E3}{T} - \frac{1.4164E6}{T^2} + \frac{6.1253E7}{T^3} - \frac{2.7198E9}{T^4}$	75–745
CO_2-N_2	$B_{12} = 18.683 + \frac{1.9172E4}{T} - \frac{2.0167E7}{T^2} + \frac{3.425E9}{T^3} - \frac{2.1815E11}{T^4}$	110–400

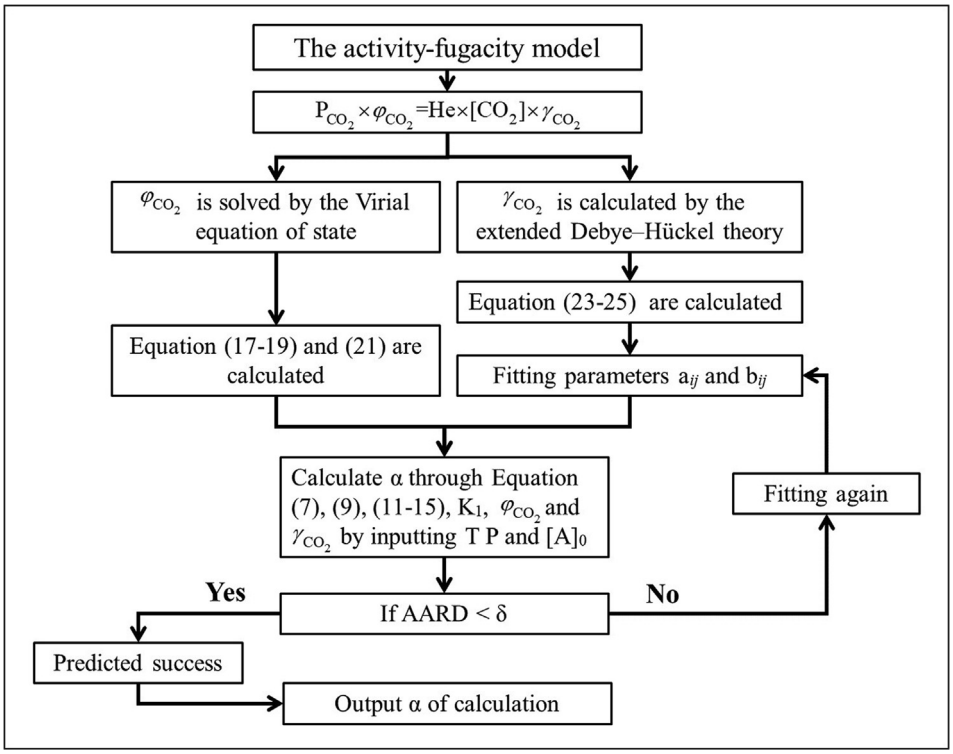

Fig. 8. Calculation progress for the fugacity-activity model.

Table 5
The binary specific-interaction coefficient β_{ij} in EMAB-H_2O-CO_2 system for the fugacity-activity model.

binary specific interaction	a_{ij} (L·mol^{-1})	b_{ij} (L·mol^{-1})
$AmineH^+$ - CO_2	−21.64	5.78E-02
$AmineH^+$ - HCO_3^-	−3.33	6.79E-03
$AmineH^+$ - CO_3^{2-}	−6.28	1.85E-02
Amine - CO_2	15.67	−4.07E-02
Amine - HCO_3^-	18.64	−4.20E-02
Amine - CO_3^{2-}	69.23	−1.97E-01
CO_2 - HCO_3^-	19.40	−5.21E-02
CO_2 - CO_3^{2-}	36.26	−1.04E-01
CO_3^{2-}- HCO_3^-	15.94	−5.77E-02
$AmineH^+$- Amine	−31.97	8.22E-02

The introduction of activity and fugacity allowed the model to be applied to different organic amine systems, and the range of experimental conditions that can be adapted is also greatly improved in this study.

The comprehensive study of these models shows that the accuracy of the semi empirical model prediction results depends on the research systems and experimental conditions. The semi empirical model is relatively easy to implement, but its application range is limited. The fugacity-activity model can be applied to various systems and is able to maintain accurate prediction results. This model is difficult to realize because of its complicated calculation, while it has a better prediction result and wider application scope. All told, the appropriate model should be selected for each different research system and experimental conditions.

4.5. Heat of CO_2 absorption in aqueous EMAB solutions

Absorption heat of CO_2 with aqueous alkanolamine solution is also critical for the design and operation of devices because it directly affects the energy requirements of the amine regeneration stage (Kim and Svendsen, 2007; Liu et al., 2017a; Zhang et al., 2020). Reducing the regeneration energy consumption can significantly improve the economic benefit and enhance the potential for industrial application. Thus, the ΔH_{abs} is one of the critical factors in the characterization of the potential new carbon dioxide capture absorbents. Usually, there are two ways to get the ΔH_{abs} into the aqueous amine solution: measurement by reaction calorimeter, and calculation by the Clausius-Clapeyron equation (Eq. (28)).

$$\frac{d\ \ln(P_{CO_2})}{d(1/T)} = -\frac{\Delta H_{abs}}{R} \tag{28}$$

whereΔH_{abs} indicates the heat of CO_2 absorption (kJ/mol) and R stands for the universal gas constant J/(mol·K).

Numerous studies conducted by Sema et al. (2011) and Rho et al. (1997) have shown that Clausius-Clapeyron can give reasonable calculation results. The measured and experimental absorption heat data of MEA, DEA and MDEA are tabulated in S-Table 6 in the Supporting Information and applied to validate the method reliability. In order to calculate the ΔH_{abs} accurately, a large number of accurate experimental data need to be used. The new fugacity-activity model can accurately predict the solubility of equilibrium CO_2 and provide an extensive solubility database. The ΔH_{abs} of EMAB was calculated from Eq.28 as the slope by plotting $\ln P_{CO_2}$ vs. 1/T using appropriate data points in the database established by the fugacity-activity model in this work. Fig. 12 shows the CO_2 absorption heats of aqueous EMAB solutions over the CO_2 loading range of 0.84–0.97 mol/mol, and the average heat of CO_2 absorption is −46.3 ± 1.1 kJ/mol.

4.6. Comprehensive evaluation and analysis of 4-(ethyl-methyl-amino)-2-butanol (EMAB) for CO_2 absorption

In order to complete the overall evaluation and analysis of the performance of 4-(ethyl-methyl-amino)-2-butanol (EMAB) as a potential efficient solvent for CO_2 capture, a comparison of EMAB

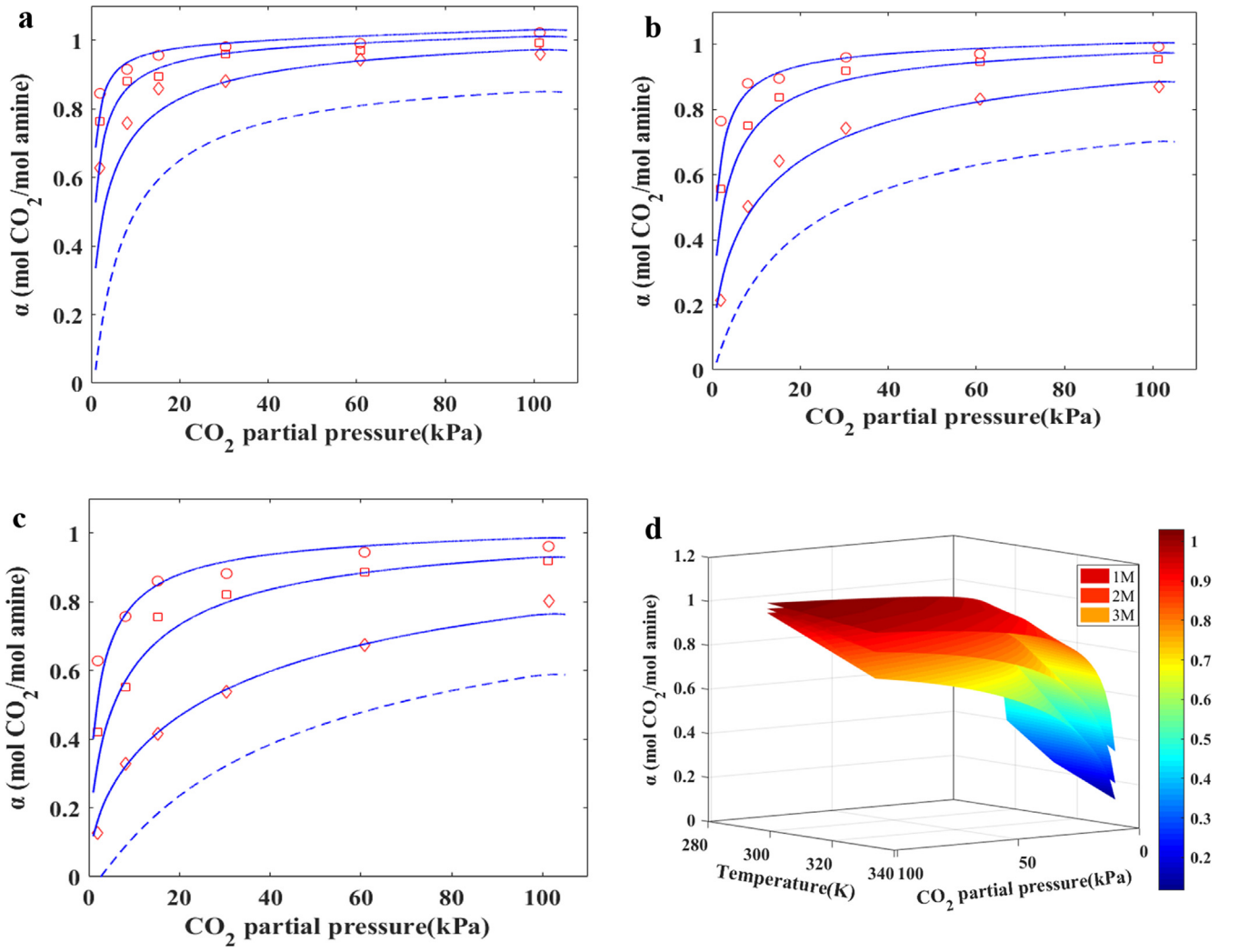

Fig. 9. Equilibrium CO_2 solubility in aqueous EMAB solution as a function of temperature and CO_2 partial pressure. (a) 1 mol/L EMAB, (b) 2 mol/L EMAB, (c) 3 mol/L EMAB. (dots are experimental values, ○-298.15 K, □-313.15 K, ◇-333.15 K, –353.15 K; curves of (a), (b), and (c) and curved surfaces of (d) are predicted data by the fugacity-activity model).

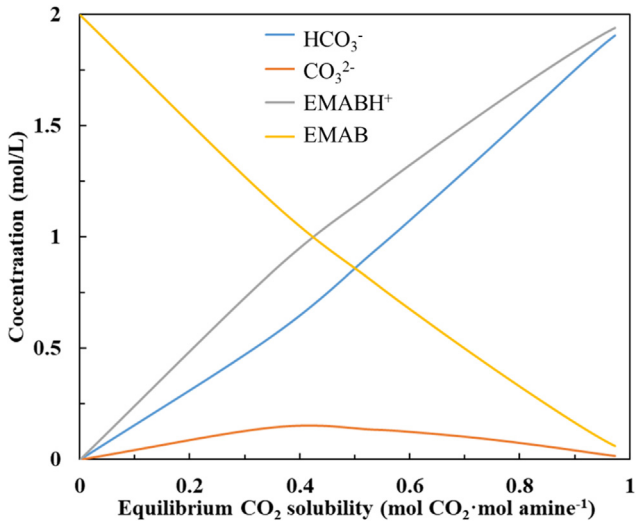

Fig. 10. Ion speciation plots of EMAB-CO_2-H_2O system at 313.15 K and 2 mol/L.

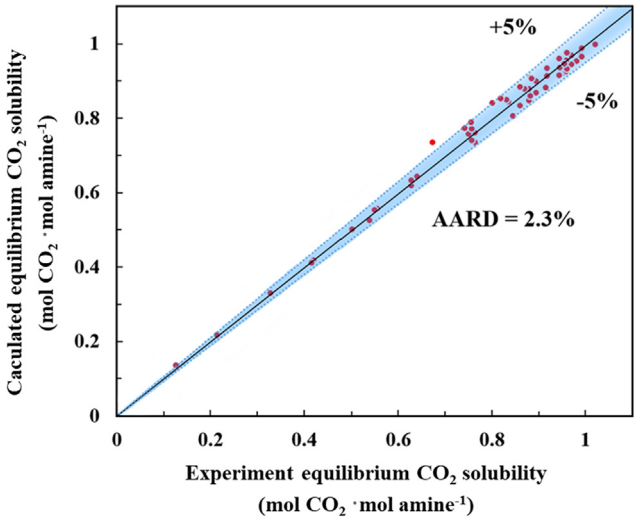

Fig. 11. Calculated equilibrium CO_2 solubility of the fugacity-activity model versus experiment equilibrium CO_2 solubility.

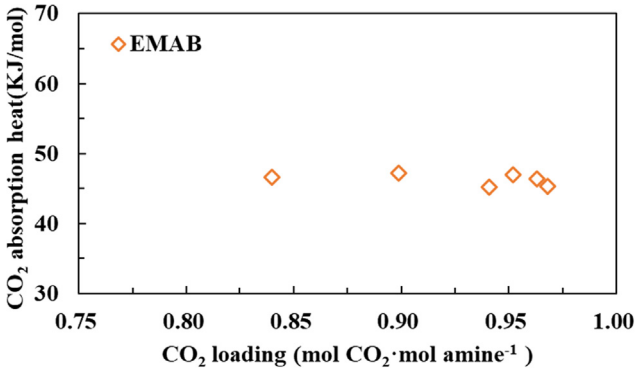

Fig. 12. The heat of CO_2 absorption in EMAB as a function of CO_2 loading at 313.15 K.

was made against other amines with respect to to CO_2 equilibrium solubility, viscosity, pKa, ΔH_{abs}, and second order rate constant (k_2).

The equilibrium CO_2 solubility of 2 mol/L EMAB solution was compared with those of 2 mol/L MEA, PZ, DEA (Haji-Sulaiman et al., 1998), AMP (Tontiwachwuthikul et al., 1991), MPDL (Xiao et al., 2017), MDEA, DEAB, and DMAB (Singto et al., 2016) at 313.15 K (Fig. 13). The current study found that the equilibrium CO_2 solubility of EMAB is higher than those of other amines (MDEA, DEA, MEA, MPDL, and AMP), but is basically the almost the same as DEAB, DMAB, and PZ under the same conditions. Piperazine (PZ) is a diamine amine, which has two nitrogen atoms, and has a relatively small molecular volume and low steric hindrance, which makes it more likely that the nitrogen atoms are close to the CO_2 molecules, resulting in a high carbon dioxide absorption capacity. It is worth mentioning that the equilibrium CO_2 solubility of di-alkyl substituted alkanolamines (i.e. EMAB, DMAB, and DEAB) was comparable to that of the diamine amine (PZ). The results show that the proper di-alkyl group in the alkanolamine structure can increase the density electron density on the N atom, thus effectively improving the equilibrium CO_2 solubility.

According to the base-catalyzed hydration mechanism, the ability of a tertiary amine to absorb CO_2 depends mainly on the ability of the nitrogen atom to capture protons, that is, on the charge density of the lone pair of electrons on the N atom. Since ethyl is a stronger electron donating group than methyl, this substituent can enhance the reactivity of the nitrogen atom to bond protons. Therefore, three kinds of amines should show the equilibrium CO_2 solubility order of DMAB < EMAB < DEAB, based on structural analysis. However, the equilibrium solubility of these three amines is almost the same. Because of the hydroxypropyl group, three amines may form the same heterocyclic structure and intramolecular hydrogen bond as shown in Fig. 1. The effect of the six-membered heterocyclic structure on the equilibrium solubility of the tertiary amine may be much greater than the effect of the alkyl substituent on the N atom, resulting in the almost same equilibrium solubility of EMAB with DMAB and DEAB.

The pKa value of EMAB was compared with some amines reported by Tagiuri et al. (2016) and Xiao et al. (2017) at 298.15 K, for some of the traditional amines and the new amines (Fig. 14). Fig. 14 shows that the dissociation constant (pKa) of EMAB is higher than that of MDEA, DEA, MPDL, DMAB, MEA, AMP, and PZ, but it is lower than that of DEAB. Obviously, di-alkyl substituted (DEAB and EMAB) alkanolamines have higher dissociation constants (pKa) and faster reaction rate with CO_2. This means that the amine structure of the β-hydroxybutyl-alkyl-alkyl group can provide a higher value of pKa. For some di-alkyl substituted alkanolamines, the pKa of EMAB (ethyl-methyl substituted amine) is larger than DMAB (dimethyl substituted amine) and smaller than DEAB (diethyl substituted amine), which can be attributed to the fact that the ethyl is a stronger electron donor than methyl, which is helpful to increase the electron density on the N atom.

The ΔH_{abs} of EMAB solution, commercially available amines (i.e. MEA, DEA, AMP (Kim et al., 2013), MDEA (Rho et al., 1997), PA (Liu et al., 2012)) and alternative/synthetic amines (i.e. MPDL (Xiao et al., 2017), DEAB, DMAB (Singto et al., 2016)) can be compared in Table 6. The results of this study indicate that the ΔH_{abs} in aqueous EMAB solution is lower than that of many commercially available amines (MEA, DEA, MDEA, PA, AMP). This is mainly attributed to the fact that the tertiary amines do not form the carbamate in amine solution and this results in a low reaction heat. Then, it was found that EMAB displays lower ΔH_{abs} than MDEA and MPDL because the bonding strength of EMAB with CO_2 is less than that of either MDEA or MPDL. In addition, in comparison with new tertiary amines DEAB and DMAB, the ΔH_{abs} in aqueous EMAB solutions was clearly higher than DMAB, and lower than DEAB. This can be attributed to the ethyl substituent on the nitrogen atom increasing the reaction heat while the methyl substituent reduces the reaction heat. To summarize, the ΔH_{abs} results can be sorted as: MEA > PZ > DEA > AMP > DEAB > MDEA > MPDL > EMAB > DEAB.

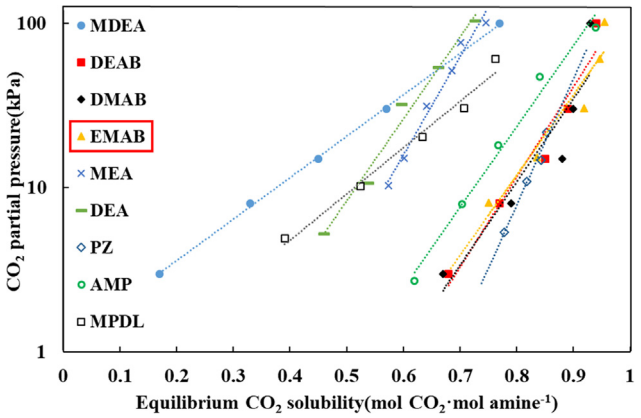

Fig. 13. The equilibrium CO_2 solubility of 2 mol/L aqueous amine solutions at 313.15 K. (The dotted line is the trend line.)

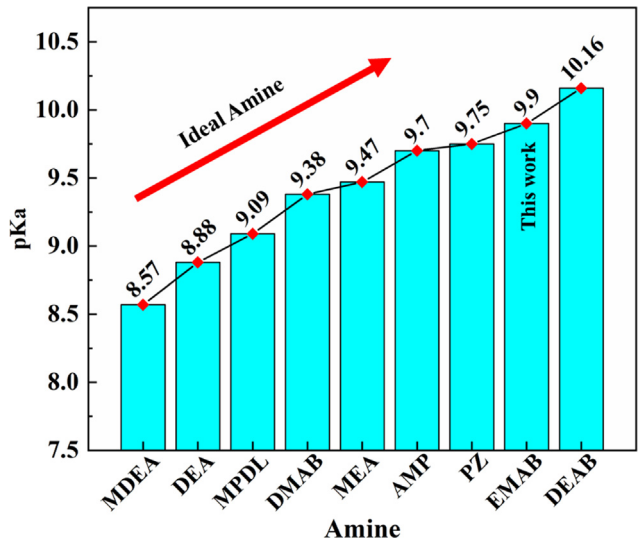

Fig. 14. The pKa of different amines at 298.15 K.

Table 6
Absorption Heats of CO_2 with different amine solutions.

Amine	Type	Structural formula	ΔH_{abs}(kJ/mol)
MEA (monoethanolamine)	primary	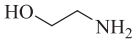	−84.3
DEA (diethanolamine)	secondary	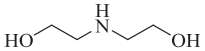	−66.9
MDEA (methyldiethanolamine)	tertiary	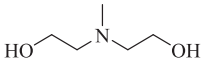	−54.6
PZ (piperazine)	cyclic	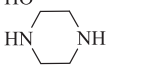	−69.7
AMP (2-amino-2-methy-1-propanol)	steric hindrance	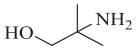	−63.95
MPDL (N-methyl-4-piperidinol)	new tertiary	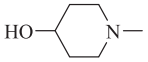	−49.1
DEAB (4-(diethylamine)-2-butanol)	new tertiary	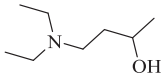	−59.76
DMAB (4-(dimethylamino)-2-butanol)	new tertiary	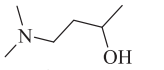	−34.17
EMAB (4-(ethyl-methyl-amino)-2-butanol)	structural design	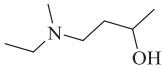	−46.3

It can be seen from Fig. 15 that the trend of second-order reaction rate constant (k_2) is MEA > DEA > AMP > EMAB > DEAB > MPDL > DMAB > PZ > MDEA at 298.15 K. As expected, the results exhibit that tertiary amine has a smaller second-order reaction rate constant (k_2) than those of the primary amine (MEA), secondary amine (DEA) and sterically hindered amines (AMP). Jamal et al. (2006), Sema et al. (2019), and Littel et al. (1992) also reported similar results. Additionally, it can be seen that k_2 of CO_2 absorption into aqueous EMAB solutions is higher than traditional tertiary amine (MDEA), new tertiary amines (e.g, DEAB, MPDL, and DMAB) and cyclic amine (PZ) solutions. Thus, it can be concluded that the reaction kinetics of the novel tertiary amine (EMAB) with CO_2 exhibits excellent CO_2 absorption performance.

From the previous discussion, it can be seen that any potential amine absorbent for the post-combustion capture requires both better absorption and desorption performance, i.e. larger CO_2 capacity (high equilibrium CO_2 solubility), fast reaction rate (higher second-order reaction rate constant k_2 value), as well lower solvent regeneration energy consumption (ΔH_{abs}). For example, the amine in the red triangle region of Fig. 16 has the above characteristics and can be used as a new generation of amine solvent. Then, the multi-angle method with consideration of the relationship of the equilibrium CO_2 solubility, second-order reaction rate constant and $\Delta H_{abs}$was applied to evaluate the CO_2 capture performances of MEA, DEA, MDEA, PZ, AMP, MPDL, DMAB, EMAB, and DEAB (Fig. 16). From Fig. 16, it can be seen that the various parameters of MEA, DEA, and AMP have the faster reaction rate but are limited by the high equilibrium CO_2 solubility and the high ΔH_{abs}; the MPDL have the low heat of CO_2 absorption but are limited by the low equilibrium CO_2 solubility and the slower reaction rate; MDEA is limited by the low equilibrium CO_2 solubility; PZ is limited by the high ΔH_{abs}; DMAB is limited by the slowly reaction rate; the equilibrium CO_2 solubility and reaction rate of EMAB and DEAB is almost the same but the ΔH_{abs} of DEAB is relatively high. The new amine EMAB performs well in all three key areas with high equilibrium CO_2 solubility, reasonably second-order reaction rate constant, and suitable ΔH_{abs}. The comprehensive analysis of equilibrium CO_2 solubility, second-order reaction rate constant (k_2), and absorption heat indicate that EMAB can be used to formulate sound CO_2 absorbents for PCC technology.

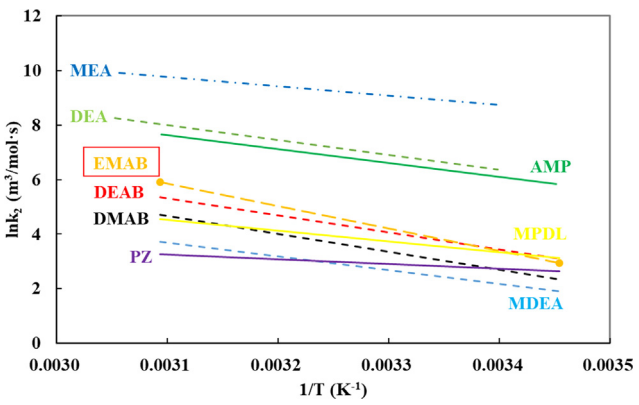

Fig. 15. The second-order reaction rate constant (k_2) of CO_2 with aqueous amine solutions. (The dotted line is the trend line.)

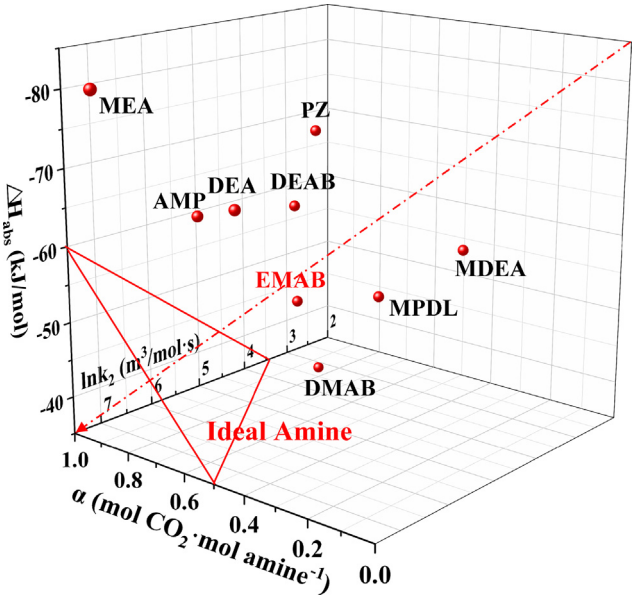

Fig. 16. A comprehensive evaluation of amines.

Also, it has been shown that methyl and ethyl within the amine structure affected the absorption heat and the rate of reaction. The ability of the amine to absorb CO_2 can be altered by adjusting the amount and location of methyl and ethyl groups, which provides guidance for the subsequent development of more potential amine capture agents. The study also displays that the accurate equilibrium solubility correlation for the tertiary amine with six-membered heterocyclic structure needs further study.

5. Conclusion

In this study, a possible potential amine 4-(ethyl-methyl-amino)-2-butanol (EMAB) was chosen for characterization based on structural analysis of di-alkyl substituted alkanolamine. The equilibrium CO_2 solubility of 1–3 mol/L aqueous EMAB solutions was measured over CO_2 partial pressure of flue gas from 2.0 to 101.3 kPa and temperature range of 298.15–333.15 K, the viscosities of CO_2 unloaded and loaded aqueous EMAB solutions of 1–3 mol/L was measured at 313.15 K, and the second-order reaction rate constant for CO_2 absorption in aqueous EMAB solution was also determined. In addition, the dissociation constant (pKa) of the aqueous EMAB solution was measured at 293.15–318.15 K and correlated with temperature according to: pKa = 2318/T + 2.12. Then, the CO_2 absorption heat (ΔH_{abs}) of the EMAB was found to be −46.3 ± 1.1 kJ/mol as calculated by the Clausius-Clapeyron equation.

For the equilibrium CO_2 solubility of aqueous EMAB solutions, the present models including Kent–Eisenberg model, Li-Shen model, Hu-Chakma model, C_f model and the novel thermodynamic models (Extended C_f model and fugacity-activity model) were used to represent the results with AARD of 9.25% for Kent–Eisenberg model, 4.74% for Li-Shen model, 12.75% for Hu-Chakma model, 8.72% for C_f model, 3.68% for Extended C_f model, and 2.3% for the fugacity-activity model. These results suggest that in general the Extended C_f model and the fugacity-activity model are able to correctly predict equilibrium CO_2 solubility in aqueous EMAB solution. Furthermore, as a result of these studies, suggestions were identified for future research of thermodynamic models for vapor-liquid equilibrium of amine-water-carbon dioxide systems.

Additionally, another critical part of this study was that the chemical–physical properties of EMAB were analyzed by a comprehensive and multi-angle method with regard to equilibrium CO_2 solubility, k_2, and ΔH_{abs}. The results indicate that the EMAB solution exhibits a suitable and excellent performance in all aspects and is a commercially available CO_2 capture agent for amine-based post combustion CO_2 capture technology.

CRediT authorship contribution statement

Qiang Li: Conceptualization, Software, Resources, Writing - original draft, Investigation. **Hongxia Gao:** Writing - review & editing, Supervision. **Sen Liu:** Data curation, Investigation. **Juan Lv:** Visualization, Investigation. **Zhiwu Liang:** .

Declaration of Competing Interest

The work described has not been published previously and is not under consideration for publication elsewhere. In addition, its publication is approved by all authors (Qiang Li, Hongxia Gao, Sen Liu, Juan Lv, Zhiwu Liang) and tacitly or explicitly by the responsible authorities where the work was carried out, and that, if accepted, it will not be published elsewhere in the same form, in English or in any other language, including electronically without the written consent of the copyright-holder.

Acknowledgment

The financial support from the National Natural Science Foundation of China (NSFC-Nos. 21536003, 21706057, 21978075 and 51521006), the Natural Science Foundation of Hunan Province in China (No. 2018JJ3033), and the China Outstanding Engineer Training Plan for Students of Chemical Engineering & Technology in Hunan University (MOE-No. 2011-40). Furthermore, the authors would like to state their great appreciation to Mr. Wilfired Olson for his assistance with a thorough upgrade of the English of the manuscript.

Appendix A. Supplementary material

Supplementary data to this article can be found online at https://doi.org/10.1016/j.ces.2020.115557.

References

Albert, A., 2012. The determination of ionization constants: a laboratory manual. Springer Science & Business Media.
Alvarez-Fuster, C., Midoux, N., Laurent, A., Charpentier, J.C., 1981. Chemical kinetics of the reaction of CO_2 with amines in pseudo m–nth order conditions in polar and viscous organic solutions. Chem. Eng. Sci. 36, 1513–1518.
Aronu, U.E., Gondal, S., Hessen, E.T., Haug-Warberg, T., Hartono, A., Hoff, K.A., Svendsen, H.F., 2011. Solubility of CO_2 in 15, 30, 45 and 60 mass% MEA from 40 to 120 °C and model representation using the extended UNIQUAC framework. Chem. Eng. Sci. 66, 6393–6406.
Böttinger, W., Maiwald, M., Hasse, H., 2008. Online NMR spectroscopic study of species distribution in MEA–H_2O–CO_2 and DEA–H_2O–CO_2. Fluid Phase Equilib. 263, 131–143.
Brönsted, J.N., Guggenheim, E.A., 1927. Contribution to the theory of acid and basic catalysis. the mutarotation of glucose. J. Am. Chem. Soc. 49, 2554–2584.
Chakraborty, A.K., Bischoff, K.B., Astarita, G., Damewood, J.R., 2002. Molecular orbital approach to substituent effects in amine-CO_2 interactions. J. American Chem. Soc. 110, 6947-–6954.
Deshmukh, R., Mather, A., 1981. A mathematical model for equilibrium solubility of hydrogen sulfide and carbon dioxide in aqueous alkanolamine solutions. Chem. Eng. Sci. 36, 355–362.
Diab, F., Provost, E., Laloué, N., Alix, P., Fürst, W., 2013. Effect of the incorporation of speciation data in the modeling of CO_2–DEA–H_2O system. Fluid Phase Equilib. 353, 22–30.
Donaldson, T.L., Nguyen, Y.N., 1980. Carbon dioxide reaction kinetics and transport in aqueous amine membranes. Ind. Eng. Chem. Fundamentals 19, 260–266.
Dreimanis, A., 1962. Quantitative gasometric determination of calcite and dolomite by using Chittick apparatus. J. Sediment. Res. 32, 520–529.
Dymond, J.H., Marsh, K.N., Wilhoit, R.C., 2003. Virial coefficients of pure gases and mixtures. Springer-Verlag, Berlin Heidelberg.
Edwards, T.J., Maurer, G., Newman, J., Prausnitz, J.M., 1978. Vapor-liquid equilibria in multicomponent aqueous solutions of volatile weak electrolytes. AIChE J. 24, 966–976.
Gao, H., Wang, N., Du, J., Luo, X., Liang, Z., 2020. Comparative kinetics of carbon dioxide (CO_2) absorption into EAE, 1DMA2P and their blends in aqueous solution using the stopped-flow technique. Int. J. Greenhouse Gas Control 94, 102948.
Haji-Sulaiman, M.Z., Aroua, M.K., Benamor, A., 1998. Analysis of Equilibrium Data of CO_2 in Aqueous Solutions of Diethanolamine (DEA), Methyldiethanolamine (MDEA) and Their Mixtures Using the Modified Kent Eisenberg Model. Chem. Eng. Res. Des. 76, 961–968.
Hu, W., Chakma, A., 1990. Modelling of equilibrium solubility of co_2 and h_2s in aqueous amino methyl propanol (AMP) solutions. Chem. Eng. Commun. 94, 53–61.
Jamal, A., Meisen, A., Jim Lim, C., 2006. Kinetics of carbon dioxide absorption and desorption in aqueous alkanolamine solutions using a novel hemispherical contactor—I. Experimental apparatus and mathematical modeling. Chem. Eng. Sci. 61, 6571–6589.
Kent, R.L., Elsenberg, B., 1976. Better data for amine treating. Hydrocarbon Process 55, 87–90.
Kim, I., Svendsen, H.F., 2007. Heat of Absorption of Carbon Dioxide (CO_2) in Monoethanolamine (MEA) and 2-(Aminoethyl)ethanolamine (AEEA) Solutions. Ind. Eng. Chem. Res. 46, 5803–5809.
Kim, Y.E., Lim, J.A., Jeong, S.K., Yoon, Y.I., Bae, S.T., Nam, S.C., 2013. Comparison of carbon dioxide absorption in aqueous MEA, DEA, TEA, and AMP solutions. Bull. Korean Chem. Soc. 34, 783–787.
Kundu, M., Mandal, B.P., Bandyopadhyay, S.S., 2003. Vapor−Liquid Equilibrium of CO_2 in Aqueous Solutions of 2-Amino-2-methyl-1-propanol. J. Chem. Eng. Data 48, 789–796.
Liang, Z., Rongwong, W., Liu, H., Fu, K., Gao, H., Cao, F., Zhang, R., Sema, T., Henni, A., Sumon, K., Nath, D., Gelowitz, D., Srisang, W., Saiwan, C., Benamor, A., Al-Marri, M., Shi, H., Supap, T., Chan, C., Zhou, Q., Abu-Zahra, M., Wilson, M., Olson, W., Idem, R., Tontiwachwuthikul, P., 2015. Recent progress and new developments

in post-combustion carbon-capture technology with amine based solvents. Int. J. Greenhouse Gas Control 40, 26–54.
Littel, R.J., Versteeg, G.F., Van Swaaij, W.P., 1992. Kinetics of CO_2 with primary and secondary amines in aqueous solutions—I. Zwitterion deprotonation kinetics for DEA and DIPA in aqueous blends of alkanolamines. Chem. Eng. Sci. 47, 2027–2035.
Liu, H., Gao, H., Idem, R., Tontiwachwuthikul, P., Liang, Z., 2017a. Analysis of CO_2 solubility and absorption heat into 1-dimethylamino-2-propanol solution. Chem. Eng. Sci. 170, 3–15.
Liu, H., Li, M., Idem, R., Tontiwachwuthikul, P., Liang, Z., 2017b. Analysis of solubility, absorption heat and kinetics of CO_2 absorption into 1-(2-hydroxyethyl)pyrrolidine solvent. Chem. Eng. Sci. 162, 120–130.
Liu, J., Wang, S., Svendsen, H.F., Idrees, M.U., Kim, I., Chen, C., 2012. Heat of absorption of CO_2 in aqueous ammonia, piperazine solutions and their mixtures. Int. J. Greenhouse Gas Control 9, 148–159.
Liu, S., Gao, H., Luo, X., Liang, Z., 2019. Kinetics and new mechanism study of CO_2 absorption into water and tertiary amine solutions by stopped-Flow technique. AIChE J. 65, 652–661.
Mann, M.E., Bradley, R.S., Hughes, M.K., 1998. Global-scale temperature patterns and climate forcing over the past six centuries. Nature 392, 779–787.
Najafloo, A., Zoghi, A.T., Feyzi, F., 2015. Measuring solubility of carbon dioxide in aqueous blends of N-methyldiethanolamine and 2-((2-aminoethyl) amino) ethanol at low CO_2 loadings and modelling by electrolyte SAFT-HR EoS. J. Chem. Thermodyn. 82, 143–155.
P. Tontiwachwuthikul, A.G.H.W., R.O. Idem, K. Maneeintr, G.J. Fan, A., Veawab, A.H., A. Aroonwilas, A. Chakma, Method of Capturing Carbon Dioxide from Gas Streams. US Patent Application, Application No. US 2011/007910078 B2, 2011.
Pérez-Salado Kamps, Á., Maurer, G., 1996. Dissociation constant of N-methyldiethanolamine in aqueous solution at temperatures from 278 K to 368 K. Journal of Chemical Engineering Data 41, 1505–1513.
Puxty, G., Rowland, R., Allport, A., Yang, Q., Bown, M., Burns, R., Maeder, M., Attalla, M., 2009. Carbon dioxide postcombustion capture: a novel screening study of the carbon dioxide absorption performance of 76 amines. Environ. Sci. Technol. 43, 6427–6433.
Rayer, A.V., Sumon, K.Z., Sema, T., Henni, A., Idem, R.O., Tontiwachwuthikul, P., 2012. Part 5c: solvent chemistry: solubility of CO_2 in reactive solvents for post-combustion CO_2. Carbon Manage. 3, 467–484.
Rho, S.-W., Yoo, K.-P., Lee, J.S., Nam, S.C., Son, J.E., Min, B.-M., 1997. Solubility of CO_2 in aqueous methyldiethanolamine solutions. J. Chem. Eng. Data 42, 1161–1164.
Sema, T., Khuenkaew, W., Sirirathomsud, O., 2019. Kinetics of CO_2 absorption in novel tertiary N-Methyl-4-piperidinol solvent. Int. J. Greenhouse Gas Control 90, 102796.
Sema, T., Naami, A., Idem, R., Tontiwachwuthikul, P., 2011. Correlations for equilibrium solubility of carbon dioxide in aqueous 4-(Diethylamino)-2-butanol solutions. Ind. Eng. Chem. Res. 50, 14008–14015.
Shokouhi, M., Jalili, A.H., Samani, F., Hosseini-Jenab, M., 2015. Experimental investigation of the density and viscosity of CO_2-loaded aqueous alkanolamine solutions. Fluid Phase Equilib. 404, 96–108.
Singh, P., Niederer, J.P.M., Versteeg, G.F., 2007. Structure and activity relationships for amine based CO_2 absorbents-I. Int. J. Greenhouse Gas Control 1, 5–10.
Singh, P., Niederer, J.P.M., Versteeg, G.F., 2009. Structure and activity relationships for amine-based CO_2 absorbents-II. Chem. Eng. Res. Des. 87, 135–144.
Singto, S., Supap, T., Idem, R., Tontiwachwuthikul, P., Tantayanon, S., 2017. The effect of chemical structure of newly synthesized tertiary amines used for the post combustion capture process on carbon dioxide (CO_2): kinetics of CO_2 absorption using the stopped-flow apparatus and regeneration, and heat input of CO_2 regeneration. Energy Procedia 114, 852–859.
Singto, S., Supap, T., Idem, R., Tontiwachwuthikul, P., Tantayanon, S., Al-Marri, M.J., Benamor, A., 2016. Synthesis of new amines for enhanced carbon dioxide (CO_2) capture performance: the effect of chemical structure on equilibrium solubility, cyclic capacity, kinetics of absorption and regeneration, and heats of absorption and regeneration. Sep. Purif. Technol. 167, 97–107.
Tagiuri, A., Mohamedali, M., Henni, A., 2016. Dissociation constant (pKa) and thermodynamic properties of some tertiary and cyclic amines from (298 to 333) K. J. Chem. Eng. Data 61, 247–254.
Tee, L.S., Gotoh, S., Stewart, W., 1966. Molecular parameters for normal fluids. Kihara potential with spherical core. Ind. Eng. Chem. Fund. 5, 363–367.
Téllez-Arredondo, P., Medeiros, M., 2013. Modeling CO_2 and H_2S solubilities in aqueous alkanolamine solutions via an extension of the cubic-two-state equation of state. Fluid Phase Equilib. 344, 45–58.
Tokarska, K.B., Gillett, N.P., 2018. Cumulative carbon emissions budgets consistent with 1.5 °C global warming. Nat. Clim. Change 8, 296–299.
Tontiwachwuthikul, P., Meisen, A., Lim, C.J., 1991. Solubility of carbon dioxide in 2-amino-2-methyl-1-propanol solutions. J. Chem. Eng. Data 36, 130–133.
Xiao, M., Cui, D., Liu, H., Tontiwachwuthikul, P., Liang, Z., 2017. A new model for correlation and prediction of equilibrium CO_2 solubility in N-methyl-4-piperidinol solvent. AIChE J. 63, 3395–3403.
Xiao, M., Liu, H., Idem, R., Tontiwachwuthikul, P., Liang, Z., 2016. A study of structure–activity relationships of commercial tertiary amines for post-combustion CO_2 capture. Appl. Energy 184, 219–229.
Xiao, M., Zheng, W., Liu, H., Tontiwachwuthikul, P., Liang, Z., 2019. Analysis of equilibrium CO_2 solubility and thermodynamic models for aqueous 1-(2-hydoxyethyl)-piperidine solution. AIChE J., 65
Zhang, Y., Que, H., Chen, C.-C., 2011. Thermodynamic modeling for CO_2 absorption in aqueous MEA solution with electrolyte NRTL model. Fluid Phase Equilib. 311, 67–75.
Zhang, R., Zhang, Y., Cheng, Y., Yu, Q., Luo, X., Li, C., Li, J., Zeng, Z., Liu, Y., Jiang, X., Hu, X.E., 2020. New Approach with Universal Applicability for Evaluating the Heat Requirements in the Solvent Regeneration Process for Postcombustion CO_2 Capture. Industrial & Engineering Chemistry Research. https://doi.org/10.1021/acs.iecr.9b05247.
Zhou, W., Jiang, D., Chen, D., Griffy-Brown, C., Jin, Y., Zhu, B., 2016. Capturing CO_2 from cement plants: A priority for reducing CO_2 emissions in China. Energy 106, 464–474.